PNAS

Supporting Information for

Design strategies for the self-assembly of polyhedral shells

Diogo E. P. Pinto, Petr Šulc, Francesco Sciortino, and John Russo

John Russo.
E-mail: john.russo@uniroma1.it

This PDF file includes:

Supporting Information Text

A. Structure details. To map the patchy particle design into a SAT problem it is necessary to translate it into boolean variables and then impose constraints such that the structures in Fig. 1 are formed.

The boolean variables can be divided into four major groups. The first group is the colour interaction variables, $x^{int}_{c_i,c_j}$, where c_i and c_j are the colour of particle i and j respectively. If this variable is true then colours c_i and c_j interact and can form a bond, otherwise not. There are a total of $(N_c)(N_c+1)/2$ of these variables. The second group is the patch colouring variable, $x^{pcol}_{p,s,c}$, where $p \in [1, N_p]$ refers to particle species, $s \in [1, V]$ to patch number and colour $c \in [1, N_c]$. If true, particle specie p has the patch number s of colour c. There are $N_p V N_c$ of these variables. Then the placement variables, $x^{L}_{l,p,o}$, where $l \in [1, L]$ refers the position of a particle in the polyhedron, $p \in [1, N_p]$ to particle specie and orientation $o \in [1, R]$. If true, a particle of species p occupies position l in the polyhedron according to orientation o. There are $N_p L R$ of these variables. Lastly, there is an auxiliary variable, $x^{A}_{l,s,c}$. If true, the particle in position l is oriented such that the patch s has a colour c. There are $V L N_c$ such variables.

The orientation mapping is given in Table I, while Tables II, III and IV present the polyhedron topology map for the icosahedron, snub cube and snub dodecahedron respectively. The patches are labeled as in Fig. 1. For the icosahedron, all patches are indistinguishable and thus they can be mapped with Table I.

There are seven main groups of clauses solved by SAT. The first guarantees that each colour can only interact with only one other colour:

$$C^{int}_{c_i,c_j,c_k} = \neg x^{int}_{c_i,c_j} \vee \neg x^{int}_{c_i,c_k} \quad [1]$$

The second ensures that patch number s of particle specie p will have exactly one colour only:

$$C^{pcol}_{p,s,c_k,c_l} = \neg x^{pcol}_{p,s,c_k} \vee \neg x^{pcol}_{p,s,c_l} \quad [2]$$

The third guarantees that position l is occupied by exactly one particle specie with one orientation:

$$C^{L}_{l,p_i,o_i,p_j,o_j} = \neg x^{L}_{l,p_i,o_i} \vee \neg x^{L}_{l,p_j,o_j} \quad [3]$$

The fourth enforces that the neighboring positions l_i and l_j connected by the patches s_i and s_j (given by the tables bellow) have colours in those patches, c_i and c_j, which interact:

$$C^{lint}_{l_i,s_i,l_j,s_j,c_i,c_j} = \neg x^{A}_{l_i,s_i,c_i} \vee \neg x^{A}_{l_j,s_j,c_j} \vee x^{int}_{c_i,c_j} \quad [4]$$

The fifth ensures that for a position l that is occupied by particle specie p with orientation o, the patch s has the right colour attributed to it:

$$\begin{aligned} C^{LS}_{l,p,o,c,s} =& (\neg x^{L}_{l,p,o} \vee \neg x^{A}_{l,s,c} \vee x^{pcol}_{p,\phi_o(s),c}) \\ & \wedge (\neg x^{L}_{l,p,o} \vee x^{A}_{l,s,c} \vee \neg x^{pcol}_{p,\phi_o(s),c}) \end{aligned} \quad [5]$$

The two last groups define multiple clauses each, the first enforces that all particle species are used, while the second enforces that all colours are used:

$$\forall p \in [1, N_p] : C^{allp.}_{p} = \bigvee_{\forall l \in [1,L], o \in [1,R]} x^{L}_{l,p,o} \quad [6]$$

$$\forall c \in [1, N_c] : C^{allc.}_{c} = \bigvee_{\forall p \in [1,N_p], s \in [1,V]} x^{pcol}_{p,s,c} \quad [7]$$

B. Thermodynamic properties. In Fig. S1 we present a study of the phase behavior of the two colour solution, C2(1), since it has the least colours and still assembles all structures. For simplicity, we restrict ourselves to the parameters $\cos\theta_{max} = 0.98$ and $\gamma = 90^\circ$, a combination which favors the snub cube structure. In panel *a* we plot the Energy-vs-density, $E(\rho)$, curve at different temperatures, where we observe a non-monotonic behavior of the average energy $E(\rho)$ with increasing density. This behaviour is characteristic of the self-assembly of finite-size aggregates (1): at low densities the system is in a gas phase of mostly monomers (unbounded particles); with increasing density particles start to aggregate and the energy decreases approaching the value $E = -5/2$ (in units of ϵ) which corresponds to an ideal gas phase of fully formed aggregates; for larger densities the gas phase competes with a percolated liquid phase that, due to geometric constraints originating from the patches arrangement on the surface of the particle, cannot form all available bonds and has thus higher energy than the gas phase. A thermodynamic motivation for the link between a $E(\rho)$ minimum and phase separation is discussed in Ref. (2). Fig. S1b shows shapshots of Monte Carlo simulations of increasing densities and at three different temperatures, displaying the transition between a gas of monomers, to a gas of snub cubes, to a percolated liquid phase.

In Fig. S1c we plot the fraction of monomers as a functions of density for the same state points as above, and additionally for the designs C4(1) and C5 at $T = 0.1$. From this, we measure the critical micelle concentration (CMC), defined as the number density at 50% of particles are in a monomeric state ($\rho_1 = 0.5$). The CMC is plotted with (green) squares in Fig. S1d,

where it is seen to have an exponential behaviour as a function of the inverse temperature, $1/T$. We also plot the points corresponding to the minima of the energy, which also show a similar exponential increase. The slope of these curves is well captured by the mean-field prediction (blue symbols) (3)

$$\rho_1 = \frac{1}{V_b} \exp[\frac{c(n)}{(n-1)} \frac{\varepsilon}{k_B T}] \quad [8]$$

where V_b is the bonding volume for the Kern-Frenkel interaction and $c(n)/(n-1)$ is the average number of bonds per particle in the clusters. Using $c(n)/(n-1)$ as a fitting parameter (4), we employ a least-squares minimization to fit the simulation results for the CMC. We find a value of $c(n)/(n-1) \approx 1.728 \pm 0.006$ best approximates the line shown in Fig. S1.

C. Yields of designs with multiple species. In Fig. S2 we show the yields measured for the designs with multiple species presented in subsection C of the SAT designs section. We show three different yield curves for the three different shells. Each curve corresponds to a different value of $\cos\theta_{max}$.

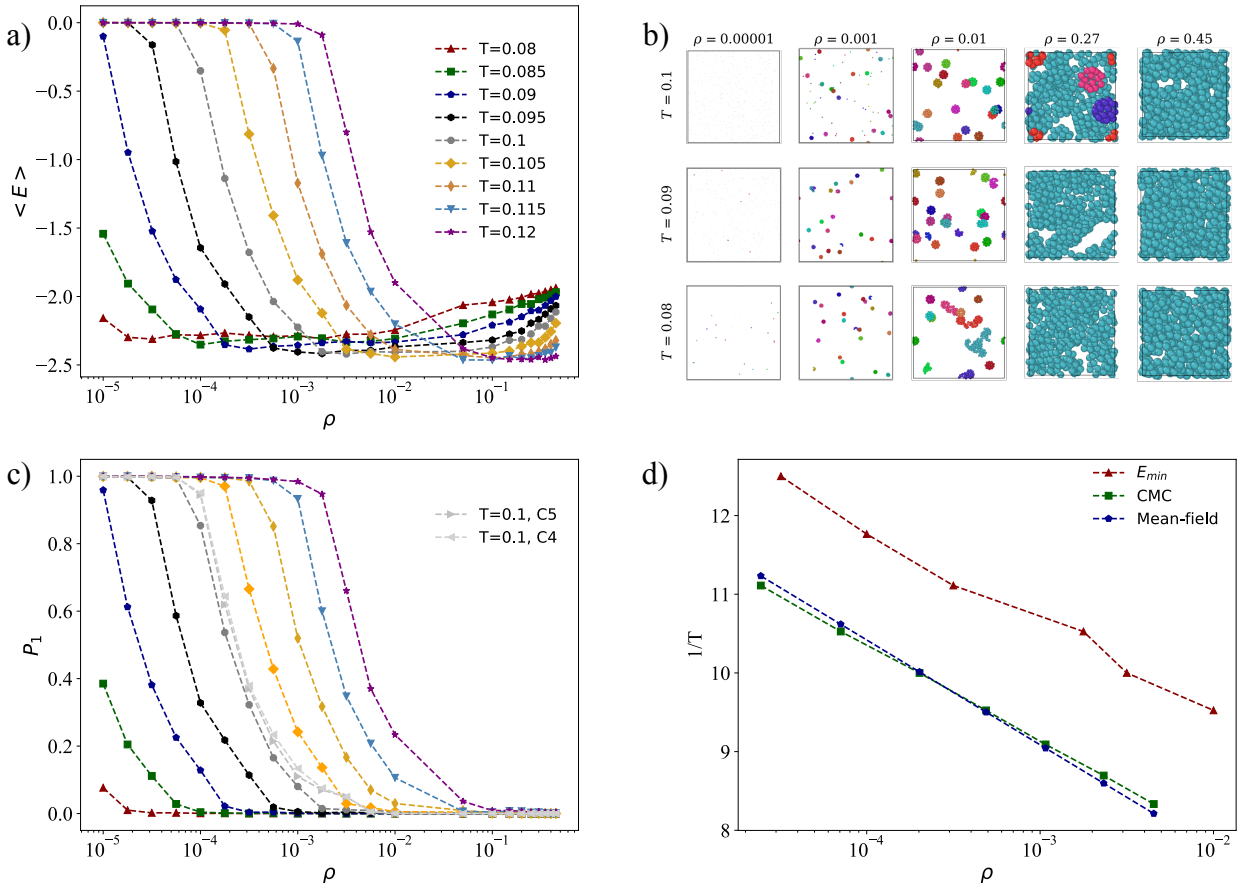

Fig. S1. a) Average potential energy per particle as a function of density for different isotherms. For clarity, the x-axis is in log-scale. We observe a non-monotonic behaviour of the average energy characteristic of self-assembly systems. b) Frontal snapshots of the system for different densities and temperatures. Images were obtained with OVITO, where the colours represent particles that belong to the same cluster. For low densities, some colours repeat themselves even though particles are not bounded due to the large number of unbounded particles which count as clusters of size one. c) Fraction of monomers as a function of the density. The color coding is the same as in a). Two new curves were added at $T = 0.1$, with a different solution (as shown in Fig. 4). d) Inverse temperature as a function of density for the point at which the fraction of monomers is equal to 50% (critical micelle concentration). A theoretical curve is drawn to estimate the CMC, it is calculated using Eq. Eq. (8). E_{min} corresponds to the energy minimum in a). All results were simulated with the one specie and two colour design (except for the two curves in the top right plot), with $\gamma = 90^\circ$ and a $\cos\theta_{max} = 0.98$.

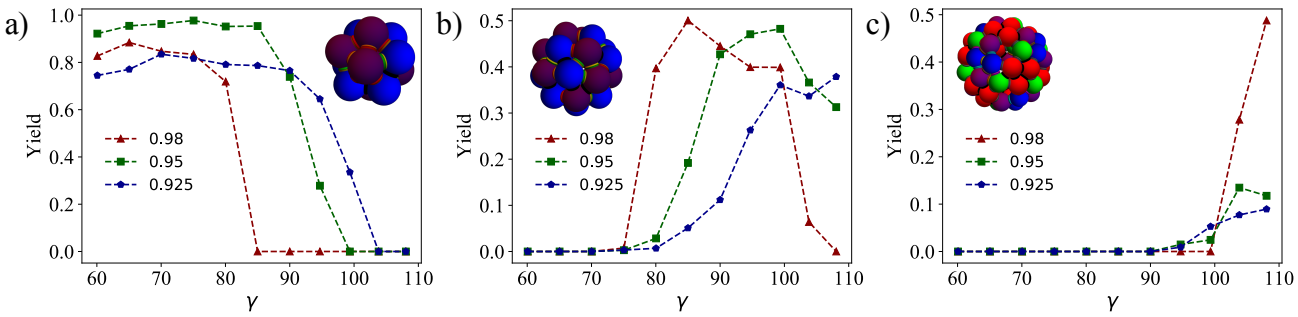

Fig. S2. Average yield of the icosahedron, snub cube and snub dodecahedron (in Fig. 1) as a function of γ (a, b and c plots respectively). These yields correspond to the results shown in Fig 5 for the designs with multiple species and mutual exclusions.

Orientation o	Mapping ϕ_o
1	(1,2,3,4,5)
2	(5,1,2,3,4)
3	(4,5,1,2,3)
4	(3,4,5,1,2)
5	(2,3,4,5,1)

Table S1. Mapping of the orientation to the patche numbers for the icosahedron.

Position l_i	Patch s_i	Position l_j	Patch s_j
1	1	3	3
1	2	9	2
1	3	5	3
1	4	6	1
1	5	10	2
2	1	4	3
2	2	11	1
2	3	7	3
2	4	8	1
2	5	12	3
3	1	7	1
3	2	9	3
3	4	10	1
3	5	8	3
4	1	5	1
4	2	11	2
4	4	12	2
4	5	6	3
5	2	6	2
5	4	9	1
5	5	11	3
6	4	12	1
6	5	10	3
7	2	8	2
7	4	11	5
7	5	9	4
8	4	10	5
8	5	12	4
9	5	11	4
10	4	12	5

Table S2. Topology of the icosahedron.

Position l_i	Patch s_i	Position l_j	Patch s_j
1	1	14	1
1	2	24	3
1	3	20	2
1	4	5	5
1	5	6	4
2	1	13	1
2	2	21	3
2	3	17	2
2	4	6	5
2	5	5	4
3	1	16	1
3	2	23	3
3	3	19	2
3	4	7	5
3	5	8	4
4	1	15	1
4	2	22	3
4	3	18	2
4	4	8	5
4	5	7	4
5	1	20	1
5	2	9	3
5	3	13	2
6	1	17	1
6	2	10	3
6	3	14	2
7	1	19	1
7	2	11	3
7	3	15	2
8	1	18	1
8	2	12	3
8	3	16	2
9	1	23	1
9	2	13	3
9	4	20	5
9	5	19	4
10	1	22	1
10	2	14	3
10	4	17	5
10	5	18	4
11	1	24	1
11	2	15	3
11	4	19	5
11	5	20	4
12	1	21	1
12	2	16	3
12	4	18	5
12	5	17	4
13	4	23	5
13	5	21	4
14	4	22	5
14	5	24	4
15	4	24	5
15	5	22	4
16	4	21	5
16	5	23	4
17	3	21	2
18	3	22	2
19	3	23	2
20	3	24	2

Table S3. Topology of the snub cube.

Position l_i	Patch s_i	Position l_j	Patch s_j
1	1	9	2
1	2	25	1
1	3	19	3
1	4	27	5
1	5	5	4
2	1	10	2
2	2	26	1
2	3	20	3
2	4	28	5
2	5	6	4
3	1	5	2
3	2	29	1
3	3	13	3
3	4	43	5
3	5	9	4
4	1	6	2
4	2	30	1
4	3	14	3
4	4	44	5
4	5	10	4
5	1	29	2
5	3	9	3
5	5	15	4
6	1	30	2
6	3	10	3
6	5	16	4
7	1	15	2
7	2	45	1
7	3	11	3
7	4	49	5
7	5	29	4
8	1	16	2
8	2	46	1
8	3	12	3
8	4	50	4
8	5	30	4
9	1	25	2
9	5	17	4
10	1	26	2
10	5	18	4
11	1	52	2
11	2	49	1
11	4	45	5
11	5	54	4
12	1	51	2
12	2	50	3
12	4	46	5
12	5	53	4
13	1	53	2
13	2	43	1
13	4	29	5
13	5	51	4
14	1	54	2
14	2	44	1
14	4	30	5
14	5	52	4
15	1	45	2
15	3	29	3
15	5	39	4
16	1	46	2

16	3	30	3
16	5	40	4
17	1	59	2
17	2	31	1
17	3	25	3
17	5	55	4
18	1	60	2
18	2	32	1
18	3	26	3
18	5	56	4
19	1	37	2
19	2	27	1
19	4	25	5
19	5	35	4
20	1	38	2
20	2	28	1
20	4	26	5
20	5	36	4
21	1	39	2
21	2	41	1
21	3	23	3
21	4	47	5
21	5	45	4
22	1	40	2
22	2	42	1
22	3	24	3
22	4	48	5
22	5	46	4
23	1	56	2
23	2	47	1
23	4	41	5
23	5	60	4
24	1	55	2
24	2	48	1
24	4	42	5
24	5	59	4
25	4	31	5
26	4	32	5
27	2	37	1
27	3	41	3
27	4	39	5
28	2	38	1
28	3	42	3
28	4	40	5
31	2	59	1
31	3	34	3
31	4	57	5
32	2	60	1
32	3	33	3
32	4	58	5
33	1	35	2
33	2	58	1
33	4	60	5
33	5	37	4
34	1	36	2
34	2	57	1
34	4	59	5
34	5	38	4
35	1	58	2
35	3	37	3
35	5	57	4

36	1	57	2
36	3	38	3
36	5	58	4
37	5	41	4
38	5	42	4
39	1	41	2
39	3	45	3
40	1	42	2
40	3	46	3
43	2	53	1
43	3	48	3
43	4	55	5
44	2	54	1
44	3	47	3
44	4	56	5
47	2	56	1
47	4	54	5
48	2	55	1
48	4	53	5
49	2	52	1
49	3	50	1
49	4	51	5
50	2	51	1
50	5	52	5
51	3	53	3
52	3	54	3
55	3	59	3
56	3	60	3
57	3	58	3

Table S4. Topology of the snub dodecahedron.

N2(1)		
Patch number	Colour	Interaction
1	A	(A,A)
2	A	(A,A)
3	A	(A,A)
4	B	(B,B)
5	B	(B,B)
N2(2)		
Patch number	Colour	Interaction
1	A	(A,A)
2	B	(B,B)
3	B	(B,B)
4	A	(A,A)
5	A	(A,A)
N3(1)		
Patch number	Colour	Interaction
1	A	(A,A)
2	A	(A,A)
3	A	(A,A)
4	B	(B,C)
5	C	(C,B)
N3(2)		
Patch number	Colour	Interaction
1	B	(B,B)
2	A	(A,A)
3	A	(A,A)
4	C	(C,C)
5	C	(C,C)
N4(1)		
Patch number	Colour	Interaction
1	B	(B,B)
2	A	(A,D)
3	D	(D,A)
4	C	(C,C)
5	C	(C,C)
N4(2)		
Patch number	Colour	Interaction
1	B	(B,B)
2	C	(C,C)
3	C	(C,C)
4	A	(A,D)
5	D	(D,A)
N5		
Patch number	Colour	Interaction
1	A	(A,A)
2	C	(C,B)
3	B	(B,C)
4	D	(D,E)
5	E	(E,D)

Table S5. Different solutions used in Fig. 4. The first column indicates the patch number, the second the colour associated with it, and the third column indicates the corresponding bond formed, the first letter corresponds to the colour of the patch and the second number to the colour it interacts with.

Icosahedron		
Patch number	Colour	Interaction
Specie 1		
1	C	(C,B)
2	F	(F,F)
3	C	(C,B)
4	F	(F,F)
5	D	(D,A)
Specie 2		
1	C	(C,B)
2	B	(B,C)
3	A	(A,D)
4	B	(B,C)
5	B	(B,C)
Snub cube		
Patch number	Colour	Interaction
Specie 1		
1	F	(F,F)
2	D	(D,A)
3	A	(A,D)
4	F	(F,F)
5	C	(C,B)
Specie 2		
1	F	(F,F)
2	D	(D,A)
3	A	(A,D)
4	B	(B,C)
5	F	(F,F)
Snub dodecahedron		
Patch number	Colour	Interaction
Specie 1		
1	K	(K,K)
2	L	(L,E)
3	D	(D,D)
4	J	(J,I)
5	H	(H,G)
Specie 2		
1	F	(F,A)
2	A	(A,F)
3	F	(F,A)
4	G	(G,H)
5	G	(G,H)
Specie 3		
1	B	(B,C)
2	K	(K,K)
3	A	(A,F)
4	H	(H,G)
5	H	(H,G)
Specie 4		
1	E	(E,L)
2	C	(C,B)
3	A	(A,F)
4	H	(H,G)
5	I	(I,J)

Table S6. Different solutions used in Fig 5. The first column indicates the patch number, the second the colour associated with it, and the third column indicates the corresponding bond formed, the first number corresponds to the colour of the patch and the second number to the colour it interacts with.

References

1. F Sciortino, A Giacometti, G Pastore, Phase Diagram of Janus Particles. *Phys. Rev. Lett.* **103**, 237801 (2009).
2. J Russo, F Leoni, F Martelli, F Sciortino, The physics of empty liquids: from patchy particles to water. *Reports on Prog. Phys.* **85**, 016601 (2022).
3. DJ Kraft, et al., Surface roughness directed self-assembly of patchy particles into colloidal micelles. *Proc. Natl. Acad. Sci. United States Am.* **109**, 10787–10792 (2012).
4. HW Hatch, SY Yang, J Mittal, VK Shen, Self-assembly of trimer colloids: effect of shape and interaction range. *Soft Matter* **12**, 4170–4179 (2016).